# Measurement of quasi-ballistic heat transport across nanoscale interfaces using ultrafast coherent soft x-ray beams

Mark Siemens[1], Qing Li[1], Ronggui Yang[1], Keith Nelson[2], Erik Anderson[3], Margaret Murnane[1] and Henry Kapteyn[1]

[1]*JILA, University of Colorado at Boulder, Boulder, CO 80309, USA*

[2]*Department of Chemistry, MIT, Cambridge, MA 02139, USA*

[3] *Center for X-Ray Optics, Lawrence Berkeley National Laboratory , Berkeley, CA 94720, USA*

**Abstract.** Understanding heat transport on nanoscale dimensions is important for fundamental advances in nanoscience, as well as for practical applications such as thermal management in nano-electronics, thermoelectric devices, photovoltaics, nanomanufacturing, as well as nanoparticle thermal therapy. Here we report the first time-resolved measurements of heat transport across nanostructured interfaces. We observe the transition from a diffusive to a ballistic thermal transport regime, with a corresponding increase in the interface resistivity for line widths smaller than the phonon mean free path in the substrate. Resistivities more than three times higher than the bulk value are measured for the smallest line widths of 65 nm. Our findings are relevant to the modeling and design of heat transport in nanoscale engineered systems, including nanoelectronics, photovoltaics and thermoelectric devices.

Rapid advances in nanoscale manufacturing have enabled control, at the quantum level, of the optical, electronic, and magnetic properties of nanostructures. Understanding thermal transport in nanostructures is very important because the flow of information and energy are often coupled [1, 2]. In particular, in the nano-electronics industry, transistors with gate widths of 45 nm are already in production, and Moore's law predicts still further reduction every two years [3]. The rapidly shrinking scale of these devices, however, fundamentally changes the way that heat is dissipated in nano devices. When the characteristic length scale ($L$) of a heat source is much smaller than the mean free path of energy carriers ($\Lambda$), heat flow becomes ballistic, and the magnitude of the heat flux deviates significantly from the Fourier law of heat conduction $q = -k \nabla(T)$, that describes normal diffusive thermal transport [1, 2].

Heat conduction beyond the Fourier regime has been studied in a number of experiments that demonstrated a reduction in thermal conductivity through nm-thickness films, superlattices, nanowires and nanocomposites [1, 2, 4-9]. However, despite its strong relevance to the practical issue of thermal management in nanoscale electronics [10], nanomanufacturing [11] and nanoparticle thermal therapy [12], the nanoscale "heat sink" problem (i.e. heat transport from a nanoscale heat source into its (bulk) surroundings) has received much less attention. When heat flows from a hotspot with dimension smaller than the phonon mean free path, the thermal energy phonon carriers travel ballistically away from the source for a significant distance before experiencing collisions, leading to a non-local (i.e. non-diffusive) thermal energy distribution [13, 14] (see Fig. 1A). The Fourier law is no longer valid at such short length scales and over-estimates the actual heat flux [1, 14]. This error can be corrected by including an additional thermal resistance, in a manner similar to what is done to account for the ballistic constriction resistance of rarefied gas [15] and electron flow [16]. Models of nanoscale heat flow have predicted such an increased thermal

resistance in the ballistic regime - however, there is currently very poor numerical agreement between different models [14, 17, 18-21].

Since phonon mean free paths in materials are in the sub-micron range even in extreme cases, experiments that address the question of ballistic transport from a nanoscale heat source must necessarily involve heated nanostructures that are coupled to a bulk substrate. The need for simultaneously high spatial and temporal resolutions make time-resolved nanoscale heat transport measurements very challenging. Moreover, the heat flow is expected to exhibit a size-dependent interface resistance, which has contributions from both a bulk interface resistance and a ballistic component from the nanoscale heat source. Sverdrup et al. used electrical resistance thermometry to measure steady-state temperature distributions in a thin 5 μm silicon membrane near a 300 nm-wide highly doped silicon resistor and observed a slight deviation from Fourier heat conduction at temperatures below 200 K [22]. However, since this experiment was not sensitive to interfacial thermal flow, it allowed a limited comparison between experiment and theory. Interface thermal flow can be very successfully measured on bulk length scales and in thin films using time-resolved optical pump-probe methods [4, 23, 24]. However, the diffraction limit for the probe light limits this technique to structures with dimensions on order of ~1 micron or greater.

In this work, we use ultrafast coherent soft x-ray beams, at a wavelength of 29 nm, to directly and accurately measure the ballistic contribution to the transport of thermal energy from a nanoscale heat source into its surroundings. The coherent short-wavelength beams — with a wavelength more than an order-of-magnitude shorter than used in past experiments in this area — were generated using a high-order harmonic generation process. In this experiment, nanoscale nickel lines deposited on a transparent substrate (sapphire or silica) are heated by a visible laser pulse, making it possible to heat a confined area (see Fig. 1). The response (i.e. thermal expansion and acoustic response) is observed by monitoring the

diffraction of a coherent soft x-ray beam from the nanostructure. This allows us to observe heat propagation through the interface and into the substrate. When the size of the interface ($L$) is much larger than the phonon mean free path ($\Lambda$), our measurement yields the bulk thermal boundary resistivity, as can be measured in a typical transient thermal reflectance (TTR) experiment [4, 23, 24]. However, at the smallest line widths of 65 nm, the interface dimension is much smaller than the phonon mean free path in the sapphire substrate ($L << \Lambda \approx 120$ nm). In this case, we measure an interfacial resistivity that is as much as three times higher than the bulk value. In contrast, measurements of heat flow in nanostructures deposited on fused-silica (with shorter mean free path $\Lambda \approx 2$ nm) yield no deviation from the bulk thermal resistivity. This confirms that we have directly observed quasi-ballistic transport of phonons in the sapphire substrate near the nanostructured interface.

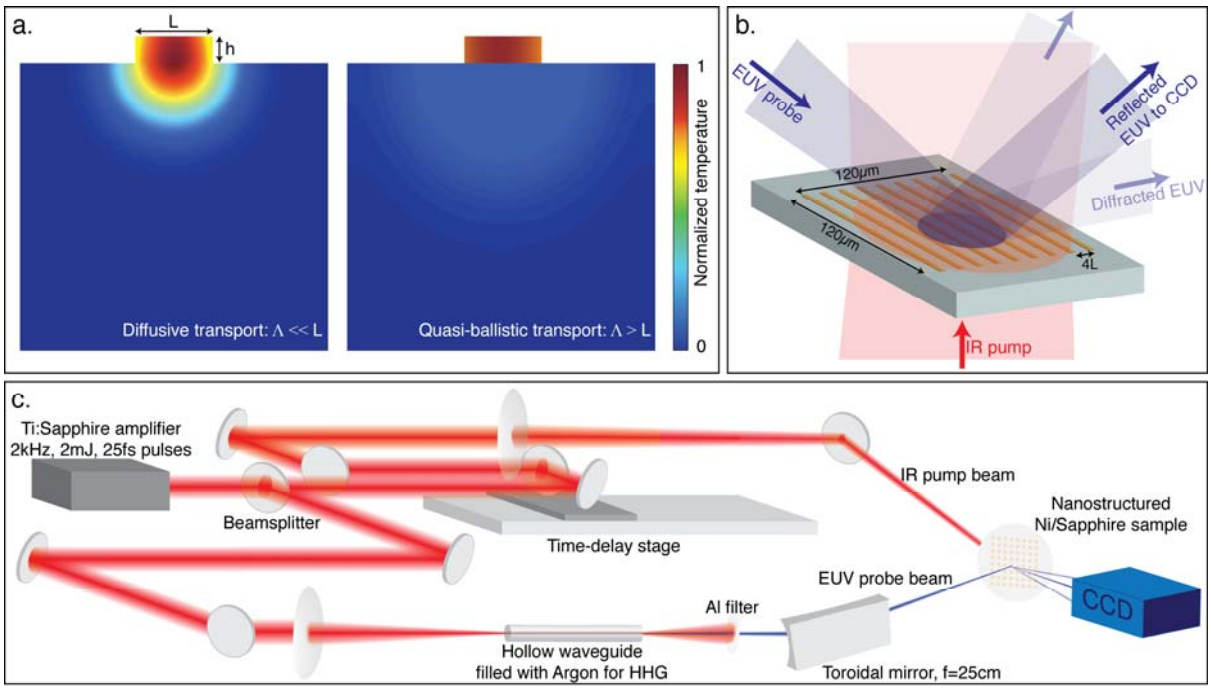


**Fig. 1.** Experimental setup for heat transport measurements through a nanoscale interface. (A) Schematic illustrating the difference between diffusive and quasi-ballistic interfacial transport. When the size of the interface is less than the phonon mean path in the substrate, Fourier diffusive heat transport breaks down. (B) Sample geometry showing IR laser illumination and soft x-ray detection scheme. (C) Experimental geometry, which uses an IR laser beam at 800 nm light to heat the nano-structure, and

soft x-ray beams at 29 nm to monitor the heat flow from the nanostructure into the substrate.

Figure 1A illustrates the difference between diffusive and ballistic heat transport, while Figs. 1B and C show the sample geometry and overall experimental setup. Nickel lines with a height of 20 nm and length 120 μm, and with widths L varying from 65 to 2000 nm, were fabricated onto a sapphire substrate using electron beam lithography and lift-off (at a fixed duty cycle of 25%). An identical sample was prepared on a fused silica reference substrate, which has a significantly shorter phonon mean free path ($\Lambda_{FS}$~2 nm at room temperature, compared with sapphire $\Lambda_{Sapp}$~ 120 nm). The nickel lines were first impulsively heated by ultrafashort, 25 fs, pulses from a high-power Ti:Sapphire laser-amplifier system [25]. Pump pulses at a wavelength of 800 nm and with an energy of ~15 μJ energy were focused to a fluence of 2.5 mJ/cm$^2$, in a spot ~5x the size of the nanostructured nickel sample to ensure uniform heating. Only the nanostructure was heated due to the high transmission of the sapphire and silica substrates to the 800 nm light.

To probe the heat flow dynamics between the nanostructure and substrate, an ultrafast, coherent, soft x-ray beam was diffracted from the nanostructure at a varying pump-probe time delays. The soft x-ray beam was generated through the high-order harmonic generation (HHG) process [26, 27] by focusing ~1 mJ pulses from the Ti:sapphire amplifier into a hollow waveguide filled with Argon gas. The resulting nonlinear interaction between the intense laser pulses and the atoms in the gas generates odd harmonics of the driving laser frequency. Absorption of the Argon gas and aluminum filters (used to block the residual 800 nm light) eliminate all but the 25$^{th}$, 27$^{th}$, and 29$^{th}$ harmonic orders, with a spectrum peaked at 29 nm. The full spatial coherence and short wavelength of the soft x-ray beams from the waveguide make it ideal for highly-sensitive interferometric measurements of nanoscale surface deformation [29, 30]. Furthermore, the very short duration of the HHG

pulses (sub-10 fs) [28] makes possible unprecedented temporal resolution for dynamics experiments. The soft x-ray harmonics are refocused onto the sample using a grazing-incidence toroidal mirror to a ~100 μm spot size. The reflected and diffracted HHG beams from the nanostructure are then recorded using a CCD camera (Fig. 1B). We then record the change in the soft x-ray probe diffraction signal as a function of delay after the IR heating pulse, as shown in Fig. 2, for varying nickel line widths. The rapid oscillations in the signal are due to surface acoustic wave (SAW) propagation in the nanostructure. Periodic surface strain caused by the patterned heating generates the SAW; we confirm that this is the source of the oscillations by comparing the measured frequency of oscillation with the Rayleigh velocity for SAW propagation in the substrate [31]. The signal of interest here, however, is the decay of the signal as the heat in the nickel nano-lines dissipates into the substrate. The rate of this thermal decay depends on the thermal conduction of the sapphire and the thermal energy transport rate across the interface between the nickel lines and the sapphire substrate.

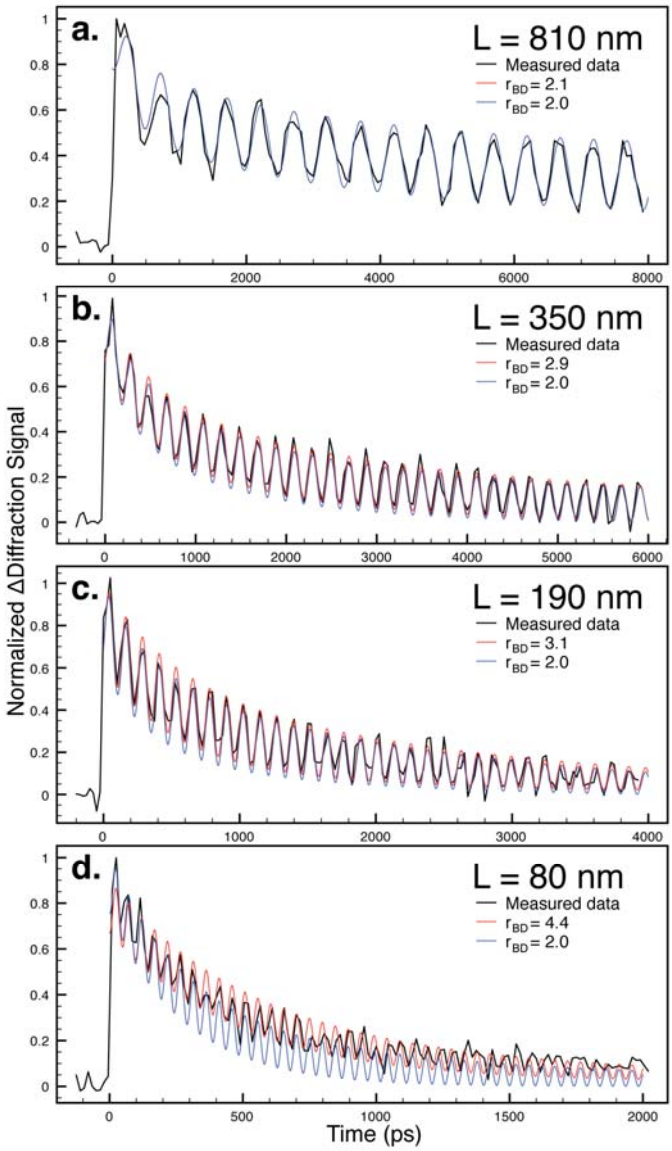


**Fig. 2.** Normalized dynamic soft x-ray diffraction signal for Ni linewidths of A. 810 nm, B. 350 nm, C. 190 nm, and D. 80 nm on sapphire. The signal in each case consists of a sharp rise due to impulsive laser heating, a thermal decay due to interfacial thermal transport, and an oscillation due to surface acoustic wave propagation. The best fit for the interface resistivity for each linewidth is shown as a red line, while the blue line shows the fit obtained by neglecting ballistic effects and simply using the bulk value. The difference between the two fits increases with decreasing linewidths.

To interpret our results, we use an analysis similar to that used for transient thermoreflectance (TTR) measurements of interfacial thermal resistivity [4, 23, 24]. In order to extract the cooling dynamics of the nickel nanostructure from data shown in Fig. 2, we used a multiphysics model including thermal transport, thermomechanics, and Fresnel optical propagation. Thermal transport across the interface is determined by the boundary condition -

$$\rho_f h C_f \frac{dT_f(x,t)}{dt} = -\frac{(T_f(x,t) - T_s(x,y=0,t))}{r_{BD}}, \quad (1)$$

where $\rho_f$ and $C_f$ are the density and volumetric specific heat in the film and $T_f$ and $T_s$ are the time and position-dependent film and substrate temperatures. Heat propagation is modeled by numerically solving the heat equation -

$$\frac{\partial T_s(x,y,t)}{\partial t} = \alpha_s \nabla^2 T_s(x,y,t) \quad (2)$$

in the substrate beneath a single nickel line, using periodic boundary conditions to account for the neighboring lines. Thermal expansion in the sapphire substrate $\Delta h_s$ is calculated from the thermoelastic equation assuming a stress-free interface [32], which involves a weighted sum over the temperature distribution at each point -

$$\Delta h_s(x_2) = 2\frac{(1+\nu_s)\alpha_s}{3\pi} \int_{x_1} \int_y T(x_1,y) \frac{y\,dx\,dy}{(x_2-x_1)^2+y^2}, \quad (3)$$

where $\alpha_s$ and $\nu_s$ are the diffusivity and coefficient of linear thermal expansion of the substrate. Fresnel optical propagation and diffraction from the resulting surface profile gives the relative signal contributions from the nickel lines and the substrate. We parameterize the results of this numerical model in terms of a total boundry resistance $r_{BD}$, and fit to the time-resolved thermal decay data. We note that we use the resistivity ($r$, units $m^2K/W$) rather than the resistance ($R$, units K/W), since the latter depends on the contact area of the interface.

At large line widths, heat is transported by phonons that undergo multiple scatterings on a length scale smaller than the dimension of the structure and therefore the Fourier diffusive heat transport model fits our data very well. This assumption cannot be expected to be valid when the dimension of the heated interface is comparable to the phonon mean free path in the substrate. The reduced scattering events in this case means that the Fourier Law over-predicts the heat flux (or under-predicts the resistivity), and therefore the heat transport should be modeled including ballistic effects. Moreover, the non-local nature of the phonon transport means that the temperature is not well defined near the interface.

To understand the nature of ballistic heat transport, we modified Chen's model for thermal flow between a nanoscale sphere and an infinite boundary [14], which calculated the diffusive and radiative components of the flux, and then combined them to obtain the total quasi-ballistic heat flux. In our case we implemented the model using a cylindrical geometry and extracted the resistivity which is inversely proportional to the heat flux. The results, shown in Fig. 3, illustrate the nature of the quasi-ballistic heat transfer effect. For large linewidths, the Fourier law predicts an increasing resistivity and the ballistic resistivity is negligible. However, for linewidths less than ≈ 100 nm, the ballistic resistivity dominates. Since our thermal model was based on Fourier diffusive heat propagation in the sample, we introduce a corrective ballistic resistance $r_B$, with an appropriate Λ/L dependence, which is extracted from the experimental data:

$$r_{BD} = r_{TBR} + r_B(\Lambda/L) \quad (4)$$

Physically, ballistic heat transport would correspond to phonons traveling from the interface and into the substrate without scattering on a length scale comparable or greater than the dimension of the interface. In our analyses, we extract the total resistivity $r_{BD}$ from the fits to our data. The bulk resistivity $r_{TBR}$ is extracted from the large linewidth measurements (L > 1 μm), while the ballistic contribution $r_B$ given by the difference between the measured and bulk values of the resistivity.

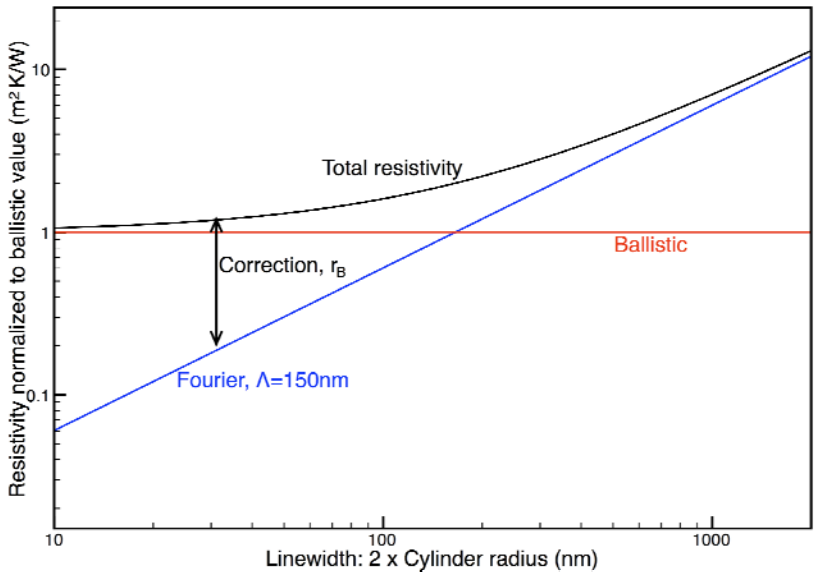


**Fig. 3.** Predicted Fourier and ballistic resistivities for heat flow from a half-cylinder. The total quasi-ballistic resistivity is the sum of the two components, and the ballistic correction term $r_B$ is measured for the first time in this experiment. The model is based on the spherical case discussed in Ref. 14

The fits to the data shown in Fig. 2 demonstrate that the measured interface resistivity increases as the heated interface gets smaller. The extracted values of the thermal interface resistivity for all linewidths deposited on both sapphire and fused silica substrates is shown in Fig. 4. As expected, large-linewidth measurements on both samples yield the bulk values of thermal interface resistivity $r_{TBR}$, as shown by the horizontal dashed lines in Fig. 3. Heat transport measurements from nanostructures into the fused silica substrate for small linewidths show a small deviation from $r_{TBR}$. This is because the phonon mean free path in fused silica $\Lambda_{FS}$~2 nm is much shorter than the smallest nickel linewidths. However, in the case of heat transfer from nanostructures deposited on sapphire substrates, the extracted values of the interface resistivity are much higher than the bulk value at the smallest linewidths— more than three times higher than the bulk value. The blue dotted and red dashed lines in Fig. 4 show the predicted resistivity values $r_B$ (proportional to $\Lambda/L$) based on Eqn. 4 for phonon mean free paths of $\Lambda_{FS}$ = 2 nm and $\Lambda_{Sa}$ = 120 nm, in excellent agreement with average phonon mean free path estimates for fused silica and sapphire.

From our data we can conclude that high harmonic based pump-probe has sufficient time and spatial resolution to measure the transient thermal behavior, including the surface acoustic wave propagation of a patterned nanostructure and that the thermal interface resistivity increases as the nanostrcture characteristic length shrinks below the mean free phonon path length of the substrate. Our quantitative measurement of the ballistic resistivity surrounding a nanoscale heat source is particularly significant for nanoelectronics, thermoelectrics and photovoltaics because the strength of the ballistic resistivity is proportional to the Knudsen number $\Lambda/L$. Therefore, ballistic effects are expected to get even stronger for silicon substrates with even longer mean free paths ($\Lambda_{Si}$ ~ 250 nm) and must be included in heat sink models.

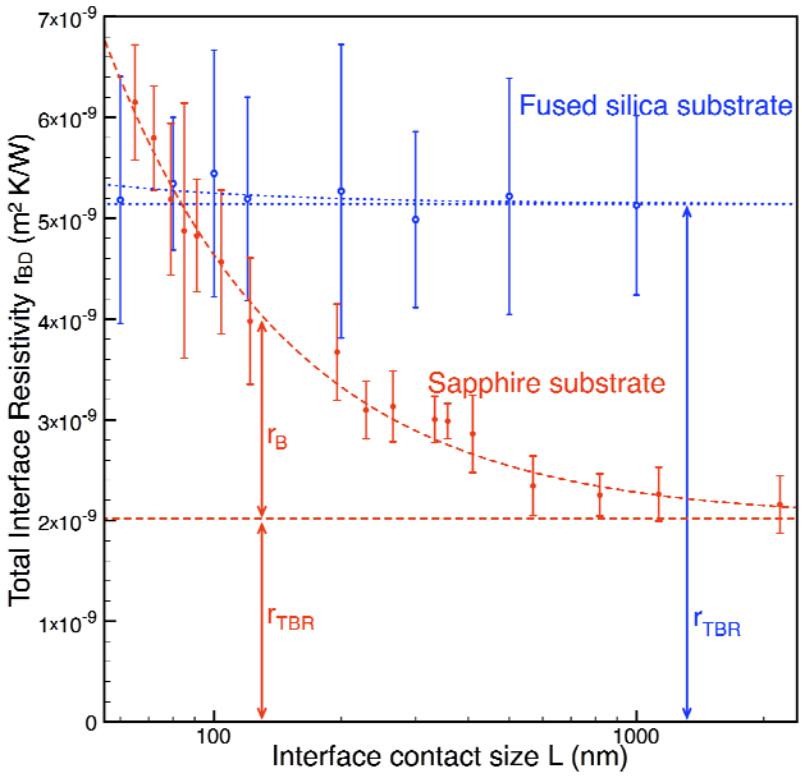


**Fig. 4.** Measured thermal interface resistivity for nickel nanostructures of width $L$ on fused silica (blue hollow dots) and sapphire (red solid dots) substrates. The blue dotted and red dashed curves show model predictions assuming $\Lambda_{FS}$ = 2 nm and $\Lambda_{Sa}$ = 120 nm, respectively.

In summary, we have observed the transition from diffusive to quasi-ballistic heat transport from nanoscale interfaces into a substrate. Quasi-ballistic heat transport dominates when the dimension of the interface is smaller than the phonon mean free path in the substrate. We measured the interfacial ballistic resistivity for various linewidths and found that for linewidths of order or less than the phonon mean free path in the sapphire substrate, the quasi-ballistic interface resistivity can be up to three times higher than the bulk value. Our data is in excellent agreement with analytical models that combine ballistic and diffusive contributions to the thermal transport, providing reliable benchmark nanoscale resistivity measurements for the numerical models. These experiments advance understanding of heat transport fundamentals, and are important for the design and manipulation of nanoscale thermal transport in circuits, thermoelectrics, photovoltaics and other structures of interest in nanotechnology.

**References**


1. G. Chen, *Nanoscale Energy Transport and Conversion: A Parallel Treatment of Electrons, Molecules, Phonons, and Photons*, Oxford University Press (2005).
2. D. G. Cahill, W. K. Ford, K. E. Goodson, G. D. Mahan, A. Majumdar, H. J. Maris, R. Merlin, and S. R. Phillpot, "Nanoscale thermal transport," Journal of Applied Physics, 93:793 (2003).
3. International Technology Roadmap for Semiconductors, http://www.itrs.net
4. W. S. Capinski, H. J. Maris, T. Ruf, M. Cardona, K. Ploog, and D. S. Katzer, "Thermal-conductivity measurements of GaAs/AlAs superlattices using a picosecond optical pump-and-probe technique," Physical Reivew B 59(12):8105 (1999).
5. Y. S. Ju and K. E. Goodson, "Phonon scattering in silicon films with thickness of order 100 nm," Applied Physics Letters 74(20):3005 (1999).
6. A. A. Joshi and A. Majumdar, "Transient ballistic and diffusive phonon heat-transport in thin-films," Journal of Applied Physics 74(1):31, (1993).
7. G. Chen, "Ballistic-diffusive heat-conduction equations," Physical Review Letters, 86:2297 (2001).
8. D. Li, Y. Wu, P. Kim, L. Shi, P. Yang, and A. Majumdar, "Thermal conductivity of individual silicon nanowires," Applied Physics Letters 83:2934 (2003).
9. R.G. Yang and G. Chen, "Thermal Conductivity Modeling of Periodic Two-Dimensional Nanocomposites," Physical Review B, Vol. **69**, 195316 (1-10), (2004).
10. E.Pop, S.Sinha, and K.E. Goodson, "Heat generation and transport in nanometer-scale transistors," Proceedings of the IEEE, Vol. 94, pp. 1587 (2006).
11. J. Lee, T. Beechem, T.L. Wright, B.A. Nelson, S. Graham, W.P. King, "Electrical, Thermal and Mechanical Characterization of Silicon Cantilever Heaters," Journal of Microelectromechanical Systems, 15, 1644 (2006).

12. K. Hammad-Schifferli, J.J. Schwarts, A.T. santos, S.G. Zhang, J.M. Jacobson, "Remote electronic control of DNA hybridization through inductive coupling to an attached metal nanocrystal antenna," Nature 415, 152 (2002).

13. G. D. Mahan and F. Claro, "Nonlocal theory of thermal conductivity," Physical Review B, 38(3):1963 (1988).

14. G. Chen, "Nonlocal and nonequilibrium heat conduction in the vicinity of nanoparticles," Journal of Heat Transfer 118, 539 (1996)

15. M. Hasegawa and Y. Sone "Rarefied gas flow through a slit," Physics of Fluids A- Fluid Dynamics, 3(3):466 (1991).

16. G. Wexler "Size effect and non-local Boltzmann transport equation in orifice and disk geometry," Proceedings of the Physical Society of London, 89(566P):927 (1966).

17. R. G. Yang, G. Chen, M. Laroche and Y. Taur, "Simulation of nanoscale multidimensional transient heat conduction problems using ballistic-diffusive equations and phonon Boltzmann equation," Journal of Heat Transfer-Transactions of the ASME 127, 298 (2005).

18. S. K. Saha and L. Shi, "Molecular dynamics simulation of thermal transport at a nanometer scale constriction in silicon," Journal of Applied Physics, 101:074304 (2007).

19. M. A. Panzer and K. E. Goodson, "Thermal resistance between low-dimensional nanostructures and semi-infinite media," Journal of Applied Physics, 103, 094301 (2008).

20. S. Volz and P.-O. Chapuis "Increase of thermal resistance between a nanostructure and a surface due to phonon multireflections," Journal of Applied Physics, 103 034306 (2008).

21. P. Heino, "Multiscale Lattice-Boltzmann finite difference model for thermal conduction from nanoscale hot spots," International Journal for Multiscale Computational Engineering, 6(2):169 (2008).

22. P. G. Sverdrup, S. Sinha, M. Asheghi, S. Uma, and K. E. Goodson, "Measurement of ballistic phonon conduction near hotspots in silicon," Applied Physics Letters, 78:3331 (2001).
23. D. G. Cahill, "Analysis of heat flow in layered structures for time-domain thermoreflectance," Review of Scientific Instruments, 75(12):5119 (2004).
24. P. E. Hopkins, P. M. Norris, and R. J. Stevens, "Influence of inelastic scattering at metal-dielectric interfaces," Journal of Heat Transfer, 130(2):022401 (2008).
25. S. Backus, R. Bartels, S. Thompson, R. Dollinger, H. C. Kapteyn, and M. M. Murnane, "High-efficiency, single-stage 7-khz high-average-power ultrafast laser system," Opt. Lett. 26(7):465 (2001).
26. A. Rundquist, C. Durfee, Z. Chang, C. Herne, S. Backus, M. Murnane, and H. Kapteyn, "Phase-matched generation of coherent soft X-rays," Science 280(5368):1412 (1998).
27. C. G. Durfee, A. R. Rundquist, S. Backus, C. Herne, M. M. Murnane, and H. C. Kapteyn, "Phase matching of high-order harmonics in hollow waveguides," Phys. Rev. Lett. 83(11):2187 (1999).
28. R. Tobey, E. Gershgoren, M. Siemens, M. M. Murnane, H. C. Kapteyn, T. Feurer and K. A. Nelson, "Nanoscale Photothermal and Photoacoustic Transients probed with Extreme Ultraviolet Radiation," Applied Physics Letters 85, 564-566 (2004).
29. R. Tobey, M. Siemens, O Cohen, M. M. Murnane, H. C. Kapteyn, and K. A. Nelson "Ultrafast Extreme Ultraviolet Holography: Dynamic Monitoring of Surface Deformation," Optics Letters 32, 286 (2007).
30. L. Miaja-Avila, G. Saathoff, S. Mathias, J. Yin, C. La-o vorakiat, M. Bauer, M. Aeschlimann, M. M. Murnane, and H. C. Kapteyn, "Direct measurement of core-level relaxation dynamics on a surface-adsorbate system," Physical Review Letters, 101(4), 046101 (2008).

31. M. Siemens, Q. Li, M. Murnane, H. Kapteyn, R. G. Yang, E. Anderson, and K. Nelson, "High-Frequency Surface Acoustic Wave Propagation in Nanostructures Characterized by Coherent Extreme Ultraviolet Beams," Applied Physics Letters, (Accepted 2009).
32. M. Vicanek, A. Rosch, F. Piron, and G. Simon, "Thermal Deformation of a solid-surface under laser irradiation," Applied Physics A-Materials Science, 59(4):407 (1994).
33. This work was funded by the DOE Division of Chemical Sciences, Geosciences, and Biosciences as well as the Office of Science, Office of Basic Energy Sciences, U.S. Department of Energy, under Contract No. DE-AC02-05CH11231 and the National Science Foundation Engineering Research Center for Extreme Ultraviolet Science and Technology. RY acknowledges the support from NSF.